# Bethe Ansatz Approach to the Kondo Effect within Density-Functional Theory

Justin P. Bergfield, Zhen-Fei Liu, Kieron Burke, and Charles A. Stafford

Phys. Rev. Lett. **108**, 066801 — Published 7 February 2012

DOI: 10.1103/PhysRevLett.108.066801

# Bethe ansatz approach to the Kondo effect within density functional theory

Justin P. Bergfield, Zhen-Fei Liu, and Kieron Burke
*Departments of Chemistry and Physics, University of California, Irvine, California 92697, USA*

Charles A. Stafford
*Department of Physics, University of Arizona, 1118 East Fourth Street, Tucson, AZ 85721*
(Dated: December 8, 2011)

Transport through an *Anderson junction* (two macroscopic electrodes coupled to an Anderson impurity) is dominated by a Kondo peak in the spectral function at zero temperature. We show that the single-particle Kohn-Sham potential of density functional theory reproduces the linear transport, despite the lack of a Kondo peak in its spectral function. Using Bethe ansatz techniques, we calculate this potential for all coupling strengths, including the cross-over from mean-field behavior to charge quantization caused by the derivative discontinuity. A simple and accurate interpolation formula is also given.

It is a truth universally acknowledged that many-body effects in strongly correlated systems are not reproduced by mean-field theory. Although Kohn-Sham (KS) density functional theory (DFT) is formally exact, it is a non-interacting theory yielding only the ground-state energy and density of a system. No other information about the correlated many-body wavefunction is available. Dynamical properties, such as excitations and response functions, are also not predicted by ground-state DFT, even with the exact functional [1]. The hope is that, for weakly-correlated systems in which ground-state DFT approximations perform well for total energies, geometries, etc., the errors in such calculations are small. Nothing in the theorems of DFT guarantees that a ground-state KS calculation can describe transport correctly [2].

Consider transport through an Anderson junction [3, 4], composed of two macroscopic leads coupled to an Anderson impurity. As an integrable system, the Anderson model is a paradigm of many-body physics. It is also an accurate model of the low-energy spectrum of molecular radical-based junctions [5]. In general, transport through such an interacting nanostructure can not be described exactly by the Landauer formula [6, 7]. However, for the specific case of the Anderson model, where interactions are included only on the impurity and not in the leads, the zero-temperature linear-response conductance in the absence of magnetic field can be computed in the Landauer approach [4, 8, 9]. In Fig. 1, we show the zero-temperature transmission through an Anderson junction as a function of the energy $\varepsilon$ of the resonant level using Bethe ansatz (BA), Kohn-Sham (KS) DFT, and Hartree-Fock (HF). In the figure, $\mu$ is the chemical potential (Fermi energy) of the metal electrodes. Remarkably, the KS-DFT treatment of this problem precisely reproduces the BA transmission, apparently describing the non-perturbative Kondo effect whose spectral peak is the source of the perfect transmission when $\varepsilon < \mu < \varepsilon + U$.

The inability to describe sharp steps in transmission is a well-understood failure of standard density functional approximations. In the limit of weak coupling to the leads, the system is a prototype example where the effects of the infamous derivative discontinuity is seen [10]. For such a system, the exchange-correlation (XC) energy of the molecule is strictly linear between integer values, and so the XC potential, its functional derivative, jumps discontinuously at such values [10]. This effect has been implicated in many well-known failures of DFT approximations such as strongly-correlated systems [11], charge-transfer excitations [12], and over-estimation of the current in organic junctions [13].

In this letter, we (a) solve the Anderson junction using BA and invert the KS equations to *derive* the KS potential, (b) show that the transport calculated within KS-DFT reproduces the BA results, but only for zero temperature and weak bias, and (c) parametrize the XC potential, providing a unique interpolation formula that works for all correlation strengths. The transport and occupancy of the Anderson model are intimately related via the Friedel sum-rule, a statement equating the occupancy and the transmission phase at the Fermi energy, as has been discussed for nearly isolated resonances [14, 15] or single-mode leads [15]. Since real molecular junctions fit neither of these categories, it reopens the question of just when an accurate ground-state KS calculation will yield accurate transport.

Using BA [16, 17], we calculate the KS potential for the Anderson model, and investigate how the derivative discontinuity develops in the limit of weak impurity-lead coupling. From this solution, we extract the asymptotic scaling form of the derivative discontinuity and establish an interpolation formula for the KS potential which is accurate for all coupling strengths, computationally simple, and illustrates the crossover from mean-field behavior at strong impurity-lead coupling to charge quantization at weak coupling.

Consider a junction composed of a nanoscale central region (C) connected to two macroscopic electrodes, labeled left (L) and right (R). The Hamiltonian of the system is $\mathcal{H} = \mathcal{H}_{\rm C} + \mathcal{H}_{\rm T} + \mathcal{H}_{\rm R} + \mathcal{H}_{\rm L}$, where $\mathcal{H}_{\rm R/L}$ describe Fermi gases in the electrodes and $\mathcal{H}_{\rm T}$ describes tunnel-

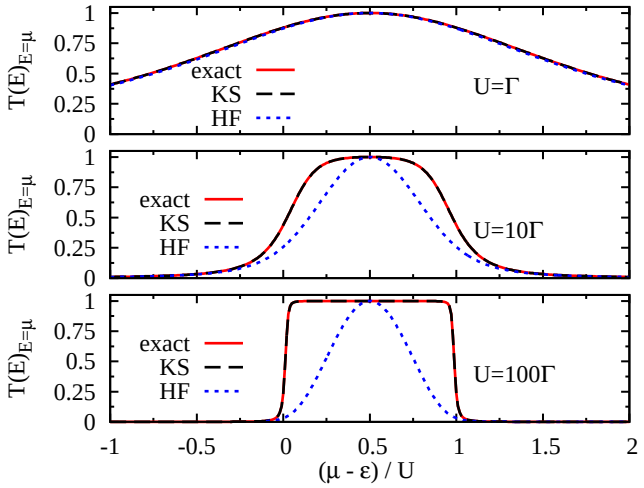


FIG. 1. (Color online) Zero-temperature transmission of an Anderson junction as a function of $\varepsilon$ using Bethe ansatz (BA), Kohn-Sham DFT (KS), and (spin-restricted) Hartree-Fock (HF). As $U$ increases, HF misses the sharp structure, but the KS transport is always the same as that from BA.

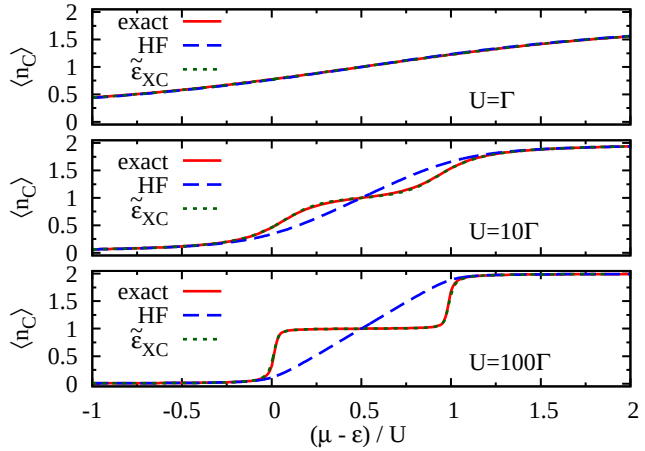


FIG. 2. (Color online) The occupancy of the Anderson junction as a function of $\mu-\varepsilon$. The BA results (solid line) exhibit discrete charge steps when $U \gg \Gamma$, whereas the mean-field RHF (dashed line) never does. The approximate occupancies calculated self-consistently within the KS-scheme using $\tilde{\varepsilon}_{\rm XC}$ [Eq. (15)] (dotted line) are nearly indistinguishable from the BA results. The BA occupancies were used to generate Fig. 1.

ing between the central region and the electrodes. The central region has the Hamiltonian [3]:

$$\mathcal{H}_{\rm C} = \varepsilon(\hat{n}_\uparrow + \hat{n}_\downarrow) + U n_\uparrow n_\downarrow, \tag{1}$$

where $\hat{n}_\sigma = d_\sigma^\dagger d_\sigma$ is the number operator for spin $\sigma$ and the charging energy $U$ is given by the Coulomb integral. The Green's function of an Anderson junction may be found using Dyson's equation in an orthonormal basis:

$$G(E) = \left[E - \varepsilon - \Sigma_{\rm C}(E) - \Sigma_{\rm T}(E)\right]^{-1}, \tag{2}$$

where $\Sigma_{\rm C}$ is the Coulomb self-energy and $\Sigma_{\rm T} \equiv \Sigma_{\rm T}^{\rm R} + \Sigma_{\rm T}^{\rm L}$ is the tunneling self-energy [18]. We consider transport in the broad-band limit where $\Sigma_{\rm T}^{\alpha}(E) = -i\Gamma^{\alpha}/2$ is pure imaginary and independent of energy, and define the mean tunneling-width $\Gamma = (\Gamma^L + \Gamma^R)/2$.

At zero temperature, the linear-response transmission function of an Anderson junction is given by [4, 17]

$$T(E)|_{E=\mu} = \Gamma^{\rm L}\Gamma^{\rm R}|G(\mu)|^2 = \frac{4\Gamma^{\rm L}\Gamma^{\rm R}}{\left(\Gamma^{\rm L}+\Gamma^{\rm R}\right)^2}\sin^2\left[\frac{\theta(\mu)}{2}\right], \tag{3}$$

where $\theta(\mu)$ is the sum of transmission eigenphases for up- and down-spin electrons evaluated at the Fermi energy $\mu = \mu_L = \mu_R$. The total number of electrons on the central impurity is related to $\theta(\mu)$ at zero temperature by the Friedel sum-rule [19–21]

$$\langle n_{\rm C}\rangle = \theta(\mu)/\pi. \tag{4}$$

In the broad-band limit, from the Bethe ansatz [16]

$$\langle n_{\rm C}(\mu)\rangle = 1 - \frac{i}{\pi\sqrt{2}}\int_{-\infty}^{\infty}\frac{d\omega}{\omega+i\eta}\frac{e^{-|\omega|/2}}{G^{(-)}(\omega)} \int_{-\infty}^{\infty} e^{i\omega(g(k)-Q)}\Delta(k)dk \tag{5}$$

with Q defined by the condition [8]

$$\frac{U-2(\mu-\varepsilon)}{\sqrt{2U\Gamma}} = \frac{i}{\sqrt{2\pi}}\int_{-\infty}^{\infty}\frac{d\omega}{\omega+i\eta}\frac{e^{-|\omega|/2-i\omega Q}}{G^{(-)}(\omega)}\frac{1}{\sqrt{-i\omega+\eta}}, \tag{6}$$

making use of the following functions

$$G^{(-)}(\omega) = \frac{\sqrt{2\pi}}{\mathbf{\Gamma}(1/2+i\omega/2\pi)}\left(\frac{i\omega+\eta}{2\pi e}\right)^{i\omega/2\pi}, \tag{7}$$

$g(k) = (k+\mu-U/2)^2/(2U\Gamma)$, and $\Delta(k) = (1/\pi)\Gamma/(\Gamma^2 + (k+\mu)^2)$, where $\mathbf{\Gamma}(x)$ is the Gamma function and $\eta = 0^+$. $\langle n_{\rm C}\rangle$ is plotted as a function of $\varepsilon$ in Fig. 2. [22]

The KS ansatz of DFT employs an effective single-particle description, defined to reproduce the ground-state density of the interacting system. By the Hohenberg-Kohn theorem, this potential is unique if it exists (it usually does) [1]. The relationship between potential and density is fixed only in the full basis-set limit, but can be defined for lattice models. The leads of an Anderson model are non-interacting and characterized by a total charge, which remains constant. Thus we define the KS system in this extreme case as that of a non-interacting junction ($U = 0$) with an on-site potential chosen to reproduce the on-site occupancy of the interacting system.

The KS Green's function in the central region may be written as

$$G^{\rm s}(E) = \left(E - \varepsilon^{\rm s} + i\Gamma\right)^{-1}, \tag{8}$$

where $\varepsilon^{\rm s}$ is the KS potential for an electron on the impurity, and is written

$$\varepsilon^{\rm s} = \varepsilon + U\langle n_{\rm C}\rangle/2 + \varepsilon_{\rm XC}, \tag{9}$$

where the second term is the Hartree contribution and the last is the correlation potential (there are no exchange contributions). The central region of the Anderson model has no internal molecular structure so the KS lead-molecule coupling is $\Gamma$ [5], ensuring a one-to-one correspondence between density and potential [23]. For more complex systems, $\Gamma$ need not be equal to the KS lead-molecule coupling.

In a standard DFT calculation, $\varepsilon_{\rm XC}$ is approximated as a functional of the density [1]. The occupancy of the central region is

$$\langle n_{\rm C}\rangle = 2\int_{-\infty}^{\infty}\frac{dE}{2\pi}\,{\rm Im}\left[G(E)\right]^{<}, \tag{10}$$

where the "lesser" Green's function is found using the Keldysh relation [18]

$$\left[G(E)\right]^{<} = 2if(E)\Gamma\left|G(E)\right|^2, \tag{11}$$

where at zero temperature, $f(E)\equiv\Theta(\mu-E)$ and $\Theta$ is the Heaviside function. Inserting the KS Green's function and solving Eq. (10) for $\varepsilon_{\rm s}$ gives

$$\varepsilon^{\rm s} = \mu + \Gamma\cot\left(\frac{\pi}{2}\langle n_{\rm C}\rangle\right), \tag{12}$$

which defines the KS potential within the Anderson model. In the broad-band limit, $\varepsilon^{\rm s}$ only involves occupancy on the central region. The KS transmission is then

$$T^{\rm s}(E) = \frac{\Gamma^{\rm L}\Gamma^{\rm R}}{\left(E-\varepsilon^{\rm s}\right)^2+\Gamma^2}. \tag{13}$$

Plugging Eq. (12) into Eq. (13), we find that $T^{\rm s}(E)$ is identical to $T(E)$, as was shown in Fig. 1. Although this identity can be derived using, e.g., local Fermi liquid theory [4], nonetheless its significance is profound: If (and only if) a mean-field theory yields the correct occupation will it yield the correct transmission.

In an Anderson junction, the Friedel sum-rule connects the transmission at the Fermi energy to the occupancy at zero temperature. As shown in Fig. 3, the full transmission spectrum of an Anderson junction exhibits three peaks: Two Coulomb-blockade peaks of width $\sim 2\Gamma$ centered about $E\approx 0$ and $E\approx U$ and a third zero-bias Kondo peak of width $\sim k_BT_K$ pinned at $E=\mu$. In contrast, the KS-DFT transmission spectrum is a single Lorentzian of width $2\Gamma$ peaked at $E=\mu$. As indicated in the figure, the KS value is a huge overestimate anywhere more than several $k_BT_K$ away from $\mu$, implying that the ground-state KS potential does not accurately predict transport at temperatures larger than $T_K$ or for bias voltages larger than $k_BT_K/e$.

From Eqs. (3), (4), (12) and (13) it is evident that the HF errors in transmission in Fig. 1 stem from errors in the occupancies of Fig. 2. When $U\lesssim\Gamma$, HF yields accurate occupancies and transmissions. But for $U\gg\Gamma$,

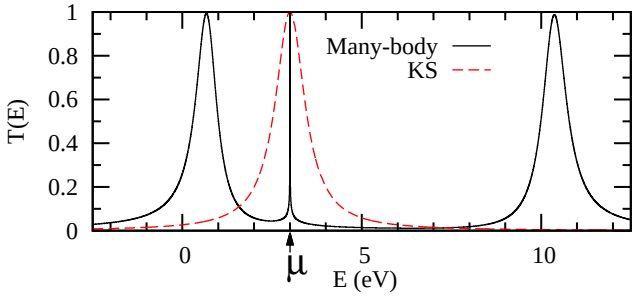


FIG. 3. (Color online) Transmission through an Anderson junction at fixed $\mu = 3eV$ with $\varepsilon = 0$, $\Gamma = 0.5eV$ and $U = 10eV$, so that $T_{\rm K} = 2mK$ [16, 17, 24]. The Doniach-Sunjic form [25] of the spectral function [26] is used near the Kondo peak, while the non-singular portion is calculated using the methods of Refs. [5, 18] with the BA occupancy. Logarithmic shifts of the charging resonances are also included [24]. More sophisticated numerical methods [27] reproduce the qualitative features shown here.

the HF occupancies lack the distinct steps present in the BA solution, causing corresponding discrepancies in the transport. Qualitatively similar errors would be found with any local or semilocal approximation for the XC potential, because such approximations are smooth functions of the interaction strength [7]. But the exact KS potential of an isolated system, infinitely weakly coupled to a reservoir, displays discontinuous jumps at integer particle number [10], just as ours does as $\Gamma/U\to 0$. The KS potential $\varepsilon^{\rm s}$ is shown as a function of occupancy in Fig. 4a for several values of $U/\Gamma$. The HF potential is linear with a slope of $U/2$. For large but finite $U/\Gamma$, the KS potential is not discontinuous but has steps (of width $\sim\Gamma/U$) corresponding to the plateaus in the occupancy, becoming discontinuous in the limit. When $U/\Gamma$ is sufficiently small there is no step in the KS potential and the HF approximation is accurate.

We now show how the step develops as $\Gamma/U\to 0$. In Fig. 4a, $\varepsilon^{\rm s}$ develops a step of height $U$ at $\langle n_{\rm C}\rangle = 1$ whose width decreases as $\Gamma/U\to 0$. Fig. 4b shows $\partial\varepsilon^{\rm s}/\partial\langle n_{\rm C}\rangle$ in the vicinity of $\langle n_{\rm C}\rangle = 1$. The horizontal and vertical axes are rescaled to illustrate the scaling behavior of the step as $\Gamma/U\to 0$. From the BA solution, as $U\to\infty$ [28]:

$$\varepsilon_{\rm XC}\simeq\frac{U}{2}\left[1-\langle n_{\rm C}\rangle-\frac{2}{\pi}\tan^{-1}\left[\frac{\pi^2U(1-\langle n_{\rm C}\rangle)}{8\Gamma}\right]\right], \tag{14}$$

whose derivative yields a Lorentzian. In Fig. 4b, we show this limit and how it is approached as $U$ grows, but notice also that the Lorentzian shape is approximately correct for all $U$ down to $\Gamma$. We thus parametrize the XC potential for $U\geq\Gamma$ by the approximate form

$$\tilde{\varepsilon}_{\rm XC} = \alpha\frac{U}{2}\left[1-\langle n_{\rm C}\rangle-\frac{2}{\pi}\tan^{-1}\left(\frac{1-\langle n_{\rm C}\rangle}{\sigma}\right)\right], \tag{15}$$

where $\alpha$ and $\sigma$ are functions of $\Gamma/U$ which $\to 1$ and $8\Gamma/(\pi^2U)$, respectively, in the limit $\Gamma/U\to 0$, and determine the amplitude and width of the correlation con-

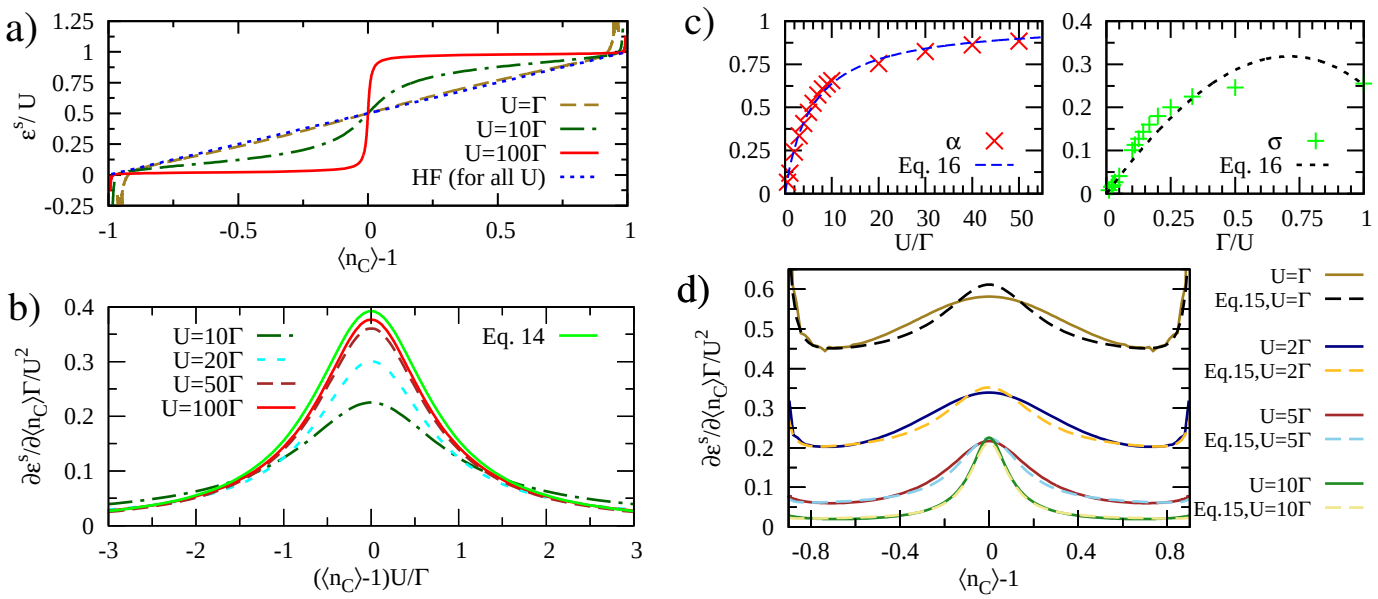


FIG. 4. (Color online) The KS potential $\varepsilon^s$ of the Anderson junction. (a) For $U \approx \Gamma$, HF is accurate; as $U$ grows, an increasingly sharp step develops, due to the *derivative discontinuity* of the exchange-correlation energy as a function of particle number. (b) $\partial\varepsilon^s/\partial\langle n_C\rangle$ for several large values of $U/\Gamma$. As $U/\Gamma \to \infty$, the exact (Lorentzian) asymptotic scaling form is recovered. (c) Exact and interpolated $\alpha$ and $\sigma$ functions are shown in the left and right-hand panels, respectively, showing the crossover from the meanfield ($U/\Gamma \sim 0$) to the strongly correlated regime ($U/\Gamma \to \infty$). The crossover from weakly to strongly correlated occurs for $U/\Gamma \approx 6$. (d) Exact and approximate $\partial\varepsilon^s/\partial\langle n_C\rangle$ spectra for several moderate $U/\Gamma$ values, highlighting the accuracy of Eq. (15). The dashed lines use Eq. (16).

tribution as a function of $\langle n_C\rangle$. Varying $\alpha$ between 0 and 1 corresponds to "turning on" charge quantization, a nonperturbative interaction effect that would not be described by any local or semilocal approximation.

To determine those parameterizations, we first note the behavior near $\langle n_C\rangle = 0,\ 2$ for $\Gamma \neq 0$. This is not generic, but stems from the restricted Hilbert space of the Anderson model. For $U/\Gamma \to \infty$, Eqs. (12) and (10) imply that $\partial\varepsilon^s/\partial\langle n_C\rangle \sim \Gamma\pi/(2\sin^2[\pi\langle n_C\rangle/2])$ near $\langle n_C\rangle = 0$. However, $3\times10^{-5}[1/\langle n_C\rangle^4]$ fits the data most accurately over the range $0.1 \le U/\Gamma \le 500$ . Precisely the same form is applied at $\langle n_C\rangle = 2$. Then a least-squares fit of Eq. (15) to the BA results, subtracting the features at $\langle n_C\rangle = 0, 2$ and limiting the fit range to $0.1 \le \langle n_C\rangle \le 1.9$, yields the values of $\alpha$ and $\sigma$ given in Fig. 4c by the points.

We also found simple fits for these functions, with

$$\alpha = \frac{U}{U + 5.68\,\Gamma}, \qquad \sigma = 0.811\frac{\Gamma}{U} - 0.390\frac{\Gamma^2}{U^2} - 0.168\frac{\Gamma^3}{U^3}. \tag{16}$$

as shown by the smooth curves in Fig. 4c. The corresponding derivatives are given by dashed curves in Fig. 4d. Eqs. (15)–(16) define an interpolation formula for the XC potential which yields the exact KS potential in both the $U/\Gamma \to 0$ and $U/\Gamma \to \infty$ limits and is accurate for all intermediate values of $U \gtrsim \Gamma$, as shown in Fig. 4. To check that our parametrization is sufficiently accurate, we performed self-consistent calculations using Eqs. (15) and (16), finding transmissions indistinguishable from those with BA occupancies for all values of $U/\Gamma$ (see Fig. 2). Our interpolation formula shows that the cross-over between weak and strong correlation occurs for $U \approx 6\Gamma$.

Our results should prove useful for the development of density functional theory in general, and for its application to transport through molecular junctions. While much is known of the consequences of the derivative discontinuity in the extreme limit of weak coupling, our results describe the entire range from strong to weak coupling, i.e., from weak to strong correlation. For transport through molecular junctions, our results provide an important specific case for which both many-body and DFT approximations can be tested. Nor are these values of $U/\Gamma$ just theoretical. For example, for the archetypal Au-[1,4]benzenedithiol single-molecule junction we find $U > 8\Gamma$, where $U$ is related to the molecule's HOMO-LUMO gap [5, 18]. In such a system, any approximate XC functional which fails to account for derivative discontinuity effects is unlikely to yield accurate results.

Note added in proof: After submission of our manuscript, Refs. 23, 29, 30 (chronological order) reporting related results appeared on arXiv. This work was supported by DOE under grant number DE-FG02-08ER46496. CAS acknowledges support from the Department of Energy under Award Number DESC0006699. KB thanks David Langreth for a decade-long conversation on the subject, and a lifetime of inspiration.

[1] R. M. Dreizler and E. K. U. Gross, *Density functional theory: An approach to the quantum many-body problem* (Springer-Verlag, Berlin, 1990).

[2] M. Koentopp, C. Chang, K. Burke, and R. Car, J. Phys.: Condens. Matter **20**, 083203 (2008).

[3] P. W. Anderson, Phys. Rev. **124**, 41 (1961).

[4] M. Pustilnik and L. Glazman, J. Phys.: Condens. Matter **16**, R513 (2004).

[5] J. P. Bergfield, G. C. Solomon, C. A. Stafford, and M. A. Ratner, Nano Lett. **11**, 2759 (2011).

[6] G. Vignale and M. Di Ventra, Phys. Rev. B **79**, 014201 (2009).

[7] M. Koentopp, K. Burke, and F. Evers, Phys. Rev. B **73**, 121403 (2006).

[8] R. M. Konik, H. Saleur, and A. Ludwig, Phys. Rev. B **66**, 125304 (2002).

[9] U. Gerland, J. von Delft, T. A. Costi, and Y. Oreg, Phys. Rev. Lett. **84**, 3710 (2000).

[10] J. P. Perdew, R. G. Parr, M. Levy, and J. L. Balduz, Phys. Rev. Lett. **49**, 1691 (1982).

[11] P. Mori-Sanchez, A. J. Cohen, and W. T. Yang, Phys. Rev. Lett. **102**, 066403 (2009).

[12] N. T. Maitra, J. Chem. Phys. **122**, 234104 (2005).

[13] F. Evers, F. Weigend, and M. Koentopp, Phys. Rev. B **69**, 235411 (2004).

[14] P. Schmitteckert and F. Evers, Phys. Rev. Lett. **100**, 086401 (2008).

[15] H. Mera and Y. M. Niquet, Phys. Rev. Lett. **105**, 216408 (2010).

[16] P. B. Wiegmann and A. M. Tsvelick, Journal of Physics C: Solid State Physics **16**, 2281 (1983).

[17] R. M. Konik, H. Saleur, and A. W. W. Ludwig, Phys. Rev. Lett. **87**, 236801 (2001).

[18] J. P. Bergfield and C. A. Stafford, Phys. Rev. B **79**, 245125 (2009).

[19] D. C. Langreth, Phys. Rev. **150**, 516 (1966).

[20] J. Friedel, Nuovo Cimento Suppl **7**, 287 (1958).

[21] H. Mera, K. Kaasbjerg, Y. M. Niquet, and G. Stefanucci, Phys. Rev. B **81**, 035110 (2010).

[22] Eq. (6) corrects a factor of 2 error from Eq. (5.8) of Ref. [16] (cf. Ref. [8]).

[23] F. Evers and P. Schmitteckert, ArXiv e-prints (2011), arXiv:1106.3658 [cond-mat.mes-hall].

[24] F. D. M. Haldane, Phys. Rev. Lett. **40**, 416 (1978).

[25] S. Doniach and M. Sunjic, Journal of Physics C: Solid State Physics **3**, 285 (1970).

[26] R. N. Silver, J. E. Gubernatis, D. S. Sivia, and M. Jarrell, Phys. Rev. Lett. **65**, 496 (1990).

[27] T. A. Costi, A. C. Hewson, and V. Zlatic, J. Phys.: Condens. Matter **6**, 2519 (1994).

[28] Z.-F. Liu, J. P. Bergfield, K. Burke, and C. A. Stafford, in preparation.

[29] P. Tröster, P. Schmitteckert, and F. Evers, ArXiv e-prints (2011), arXiv:1106.3669 [cond-mat.mes-hall].

[30] G. Stefanucci and S. Kurth, ArXiv e-prints (2011), arXiv:1106.3728 [cond-mat.mes-hall]; G. Stefanucci and S. Kurth, Phys. Rev. Lett. **107**, 216401 (2011).